Bulgarian Chemical Communications, Volume 53, Issue 4 (pp. 480 - 485) 2021 *DOI: 10.34049/bcc.53.4.T006*

Preliminary investigation into the synthesis and characterisation of single nucleotide polymorphs of human glutathione-*S*-transferase class PI

S. Mathura

University of the Witwatersrand, Johannesburg, South Africa

Accepted: November 13, 2021

This preliminary work probes the structure-function relationship of single nucleotide polymorphs (SNP) of human glutathione-s-transferase class pi (hGSTP1-1). To this end, two SNPs were synthesised by site-directed mutagenesis: P124A and Y80C, both in the all-helical C-terminal domain of hGSTP1-1. The mutant proteins were then expressed using standard overexpression methods; both mutants expressed fewer colonies and produced less protein relative to wildtype. Proteins were structurally characterised by spectroscopy relative to wildtype. Preliminary circular dichroism findings revealed minor alterations of the Y80C structure whilst P124A remained unchanged, relative to wildtype. Similarly, fluorescence spectroscopy findings for Y80C remained unchanged for P124A, relative to wildtype. Interestingly, thermal denaturation studies revealed destabilisation in the mutant enzymes compared to wildtype (TmWT = 55 ± 3 ºC; TmP124A = 51 ± 3 ºC; TmY80C = 47 ± 3 ºC).

Keywords: hGSTP1-1; SNP; polymorphism; structure-function relationship; detoxification proteins.

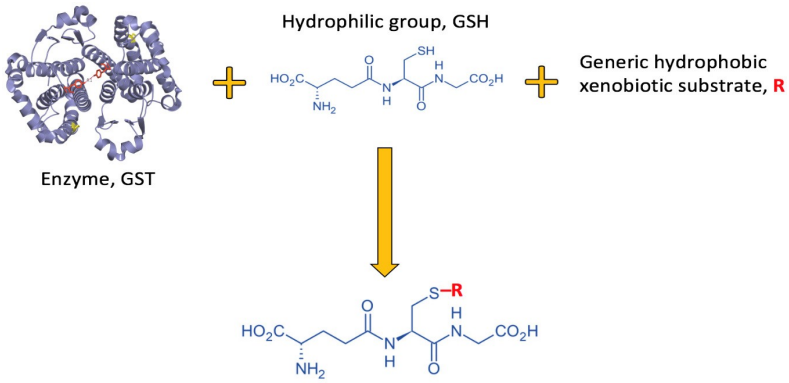

Scheme 1. Demonstrating the generic pathway for the conjugation of the phase II detoxification enzyme GST [6] to the hydrophilic group reduced glutathione (GSH) and to the xenobiotic substrate (R). Adapted from [5].

INTRODUCTION

Cytosolic glutathione-S-transferases (GSTs, E.C. 2.5.1.18, formerly called '*ligandin*') are a superfamily of multifunctional proteins. GST protein functions include both catalytic and non-catalytic roles such as redox reactions, intracellular binding of ligands, ligand transport. Of particular interest is its role as classical phase II detoxification enzyme [1-3].

As classical phase II detoxification enzymes, GSTs play a critical role in protecting the cell against oxidative stress and in the detoxification of xenobiotics [3, 4]. Cellular detoxification of xenobiotics is achieved by catalysing the covalent binding of reduced glutathione (GSH) onto nonpolar xenobiotic molecules through a nucleophilic attack mechanism. GST binds GSH and initiates the deprotonation of the sulfhydryl group. The reduced glutathione-GST complex then binds to the xenobiotic substrate (Scheme 1). The metabolised xenobiotics are then expelled through the mercapturate pathway [3-5].

Structurally, there are three main GST families: cytosolic, mitochondrial and microsomal (or MAPEG proteins). Each family comprises a number of classes (Table 1). Human GST enzymes comprise 11 classes [2, 7, 8]. This work focuses on the structure and function of canonical cytosolic human GST class Pi (hGSTP1-1). Mutations in hGSTP1-1 structure, specifically single nucleotide polymorphisms (SNP), have been linked to several human diseases and ailments [7-12]. Probing the structural integrity of hGSTP1-1 and related SNP mutations is therefore of interest as it would lend insight into the complex structure-function relationship of these enzymes.

* To whom all correspondence should be sent:
E-mail: sadhna.mathura@wits.ac.za

Table 1. GST superfamilies and classes. Human classes are underlined. Soluble mammalian classes are italicised. Human GST enzyme of interest (pi) is in bold [2, 7, 8].

GST Superfamily	Number of Classes	Class Names
Cytosolic	13	*alpha*, beta, delta, epsilon, *zeta*, *theta*, *mu*, nu, ***pi***, *sigma*, tau, phi, *omega*
Mitochondrial	1	*kappa*
Microsomal (MAPEG)	4	I, II, III, IV

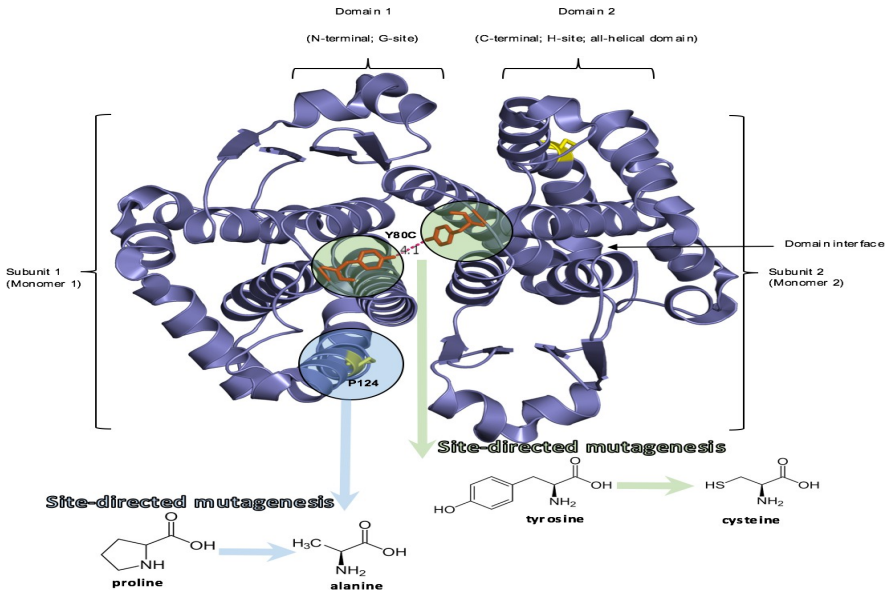

Figure 1. Quaternary structure of homodimeric hGSTP1-1 [5], indicating subunits, domains and interfaces. The highlighted regions show the SNP residues of interest in this work: P124A (blue) and Y80C (green).

Structurally, hGSTP1-1 is a homodimeric protein consisting of about 200 amino acids (Figure 1). The protein has a canonical fold comprising two distinct domains: a thioredoxin-like N-domain, and an all-helical C-domain [2, 3].

The structural GST fold is considered to have evolved from a thioredoxin/glutaredoxin common ancestor to which the all-helical C-domain was added [4]. There are two active sites: a GSH-specific G-site within the smaller N-terminal thioredoxin-like domain; and a non-specific hydrophobic substrate-binding H-site (target for xenobiotics) contained within the larger all-helical C-terminal domain.

Probing hGSTP1-1 structure-function relationship by examining SNPs has been well-characterised in the N-domain, and has provided considerable insight into the active sites, particularly the G-site [12-14]. In this work however, we will examine selected SNPs in the all-helical C-domain. Our strategy is to compare the structure of each SNP to that of wild type (WT) to elucidate how the identity of the residue at those respective positions influences the structural, catalytic and stability properties at the binding sites. This information should provide some structural evidence for the correlated diseases.

In this preliminary report, we have synthesised and structurally characterised two interesting C-domain SNPs (Figure 1):

(1) P124A which is of interest given its proximity to the subunit interface and,

(2) Y80C which is of interest given its proximity to both subunit and domain interfaces, and is highly conserved, suggesting structural significance.

EXPERIMENTAL

Mutagenesis, transformation and sequencing of mutants P124A and Y80C

hGSTP1-1 mutants, P124A and Y80C, were synthesised by site-directed mutagenesis (Stratagene QuickChange™ II, CA, United States), using recombinant plasmids that code for wildtype hGSTP1-1. Oligonucleotide primers for the mutagenesis were designed using Primer-X software [16]. Plasmid DNA was verified by sequencing analysis (Inqaba Biotechnical Industries (Pty) Ltd, Pretoria, South Africa) and aligned using BLAST [17] and 4Peaks software [18]. Plasmids were then transformed into *E. coli* T7 cells for overexpression of the mutant enzymes using standard methods [19].

Overexpression and purification mutants P124A and Y80C using standard methods

Mutant enzyme overexpression was induced using an IPTG (0.2 mM; 30°C; 8 h). The cultured cells were harvested by centrifugation, re-suspended (50 mM Tris-HCl buffer, pH 8.0; -20 °C). Purification was achieved using cobalt HisTrap™ column with binding buffer [50 mM Tris-HCl pH 8.0, 0.5 M NaCl, 50 mM imidazole (eluted with 300 mM), 0.02 % sodium azide], and analysed using SDS-PAGE [16-19].

Structural characterisation of mutants P124A and Y80C using standard methods [16]

Both far-UV circular dichroism (CD) and fluorescence emission spectra measurements were conducted with 1 μM of both wildtype and mutant enzymes in phosphate buffer (pH 7.4, 20 mM, 20 ^{o}C). Buffer also included 1mM DDT and 0.02% (w/v) NaN3. Data were recorded on a Jasco J-810 and represent an average of 10 accumulations. Fluorescence measurements were an average of three accumulations and were conducted on a Perkin-Elmer LS50B. Spectra were corrected for buffer.

RESULTS AND DISCUSSION

Synthesis data: primer design, sequencing and alignment, overexpression (SDS-PAGE)

The hGSTP1-1 mutants P124A and Y80C were synthesised to investigate the structure-function relationship of the wildtype hGSTP1-1. The first step in this process is accurate primer design in order to code for the correct single nucleotide mutation. Both the forward and reverse primers were successfully designed using Primer-X [16] for the tyrosine to cysteine, and the proline to alanine point mutations, respectively (Table 2). The underlined bases represent the coding for the mutations of interest.

The second step in the process of generating the hGSTP1-1 mutants was DNA sequencing and sequence alignment analysis to confirm that each of the selected mutations had to be achieved, as well as to confirm the absence of any other mutation (Figures 2 and 3 for mutants Y80C and P124A, respectively). Sequencing data indicate that mutant codon for tyrosine was replaced by cysteine (Figure 2) for the Y80C mutation and the proline was replaced by alanine (Figure 3). The truncated sequence alignment for mutant Y80C indicates a 99% alignment with known hGSTP1-1 wildtype protein. The same was noted for P124A. This indicates that there were no other mutations.

Following the sequencing and alignment, both mutant proteins and wildtype were overexpressed and purified using standard methods [16, 19]. Once purified, the protein was analysed by mass using SDS-PAGE analysis (Figure 4). Proteins for both wildtype and mutants were successfully expressed and purified to a single band at the anticipated mass (25 kDa). Mass for mutants was consistent with standard calibration data (Figure 4). SDS-PAGE analysis of wildtype (blue triangle) and mutants Y80C (red circle) and P124A (orange square) was plotted on the standard curve which was fitted to a straight line (R = 0.970). Equation of the fitted line is y = -0.020x + 2.203.

Characterization data: structural analysis

hGSTP1-1 and mutants were structurally characterised using both far-UV CD and fluorescence emission spectra spectroscopy to probe their secondary structure and unfolding pathways. Far-UV CD spectra show similar spectral profiles for both mutants and wildtype with peaks at 190 nm, 208 nm and 222 nm (Figure 5). There is however diminished intensity for the Y80C mutant suggesting that the chromophore is likely being shielded in some way, relative to wildtype. This observation may indicate an opening up of the structure around the chromophore.

The fluorescence emission spectra for wildtype and mutants are reported below (Figure 6). What is interesting is that we would expect the Y80C mutant to have a diminished intensity relative to wildtype given that the tyrosine has been replaced by a cysteine. However, this is not the case, suggesting that there is a possible opening up of the secondary structure to expose other fluorescent moieties on the protein. Solid state analysis would add more information here.

Table 2. Forward and reverse primers used for site directed mutagenesis of P124A and Y80C mutants of hGSTP1-1. Primers designed using Primer-X [16]

Primer	Sequence
Y80C-forward	5’-ttcaagctgggcctggactgtcccctgccctacttg-3’
Y80C-reverse	5’-caagtagggcaggggacagtccaggcccagcttgaa-3
P124A-forward	5'-cttcagttgcccggccagtgccttcacat-3'
P124A-reverse	5'-atgtgaaggcactggccgggcaactgaag-3'

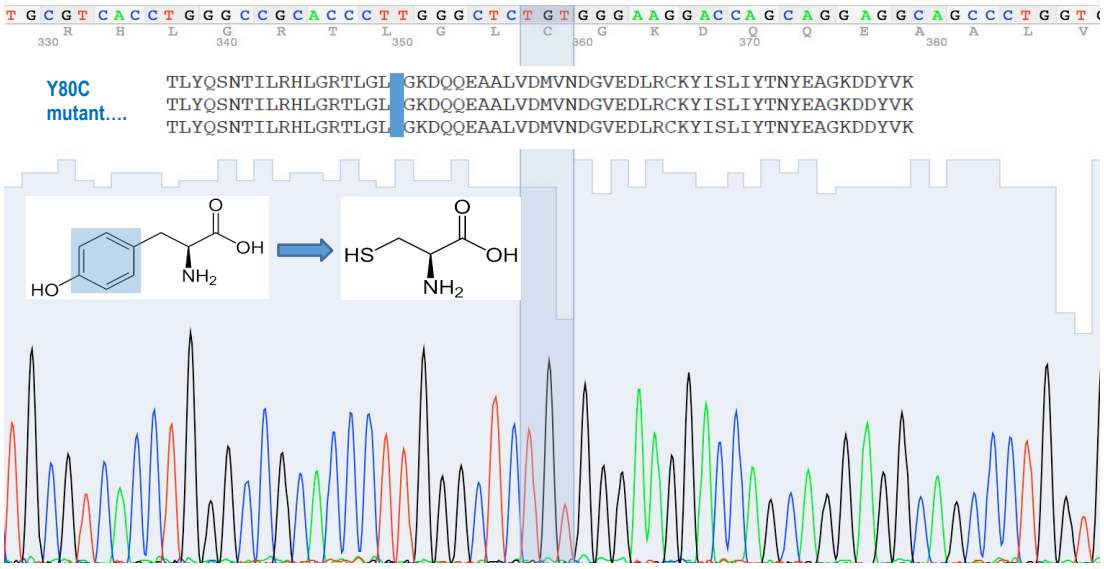

Figure 2. Sequencing data indicating mutant codon for tyrosine to cysteine replacement (highlighted in yellow) and subsequent alignment of mutant Y80C sequence against wildtype (highlighted in blue).

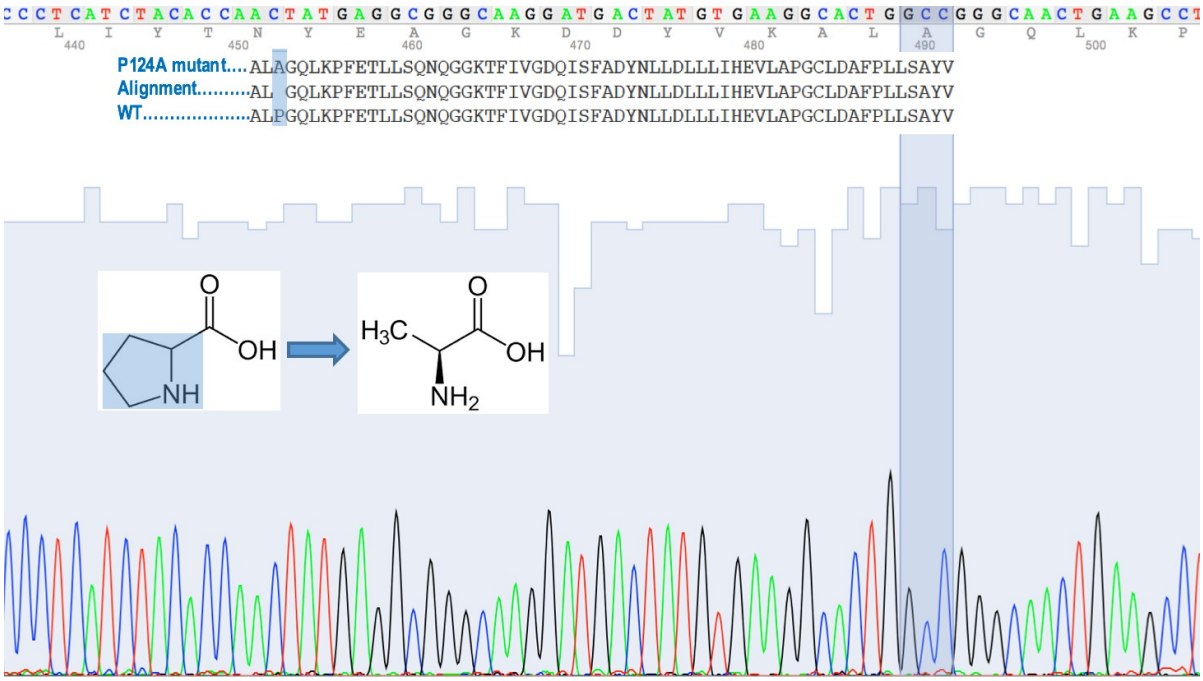

Figure 3. Sequencing data indicating the mutant codon for the proline to alanine replacement (highlighted in yellow) and the subsequent alignment of mutant P124A sequence against wildtype (highlighted in blue).

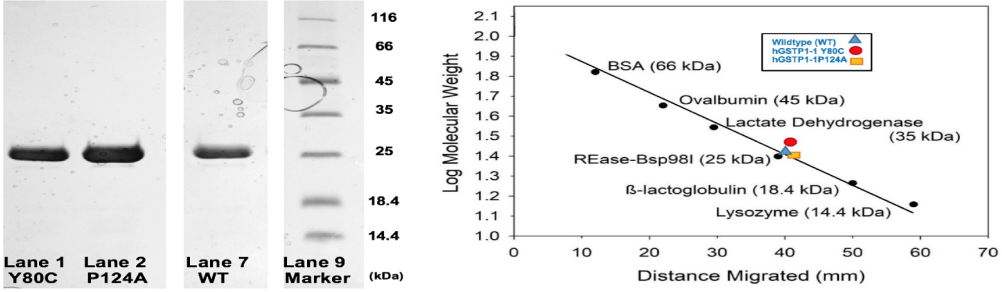

Figure 4. SDS-PAGE analysis of WT (Lane 7) and mutants Y80C (Lane 1) and P124A (Lane 2). Gel specs: 16% acrylamide; glycine; 120 V; 5 µL sample load; ~5 µg.

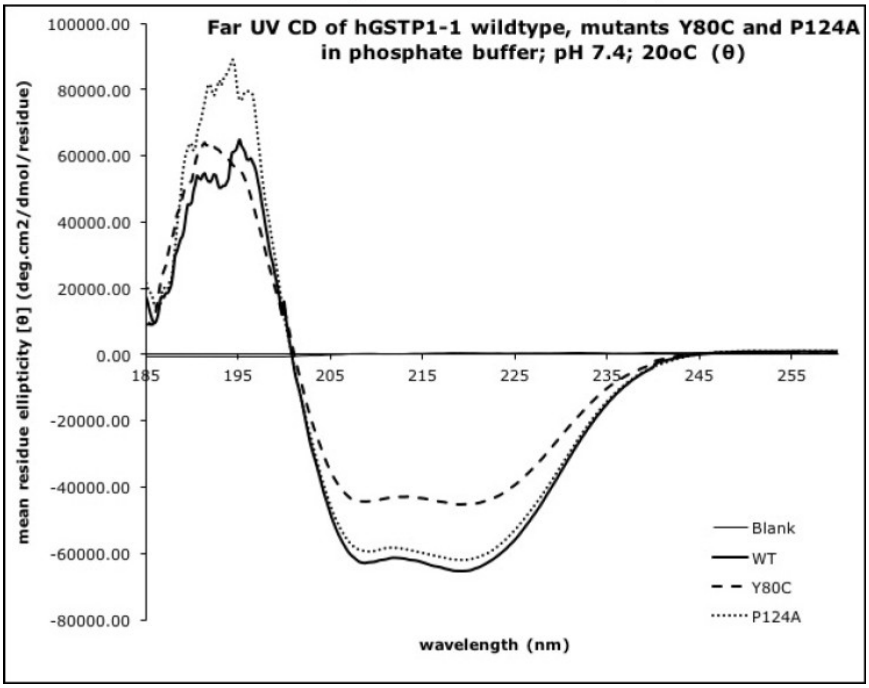

Figure 5. The resultant far-UV CD spectra for the WT dimer (5 µM) (──); mutant Y80C (5 µM) (- - -) and P124A (5 µM) (....) in 20 mM sodium phosphate buffer pH 7.4, containing 1 mM EDTA and 0.02% (w/v) NaN are shown.

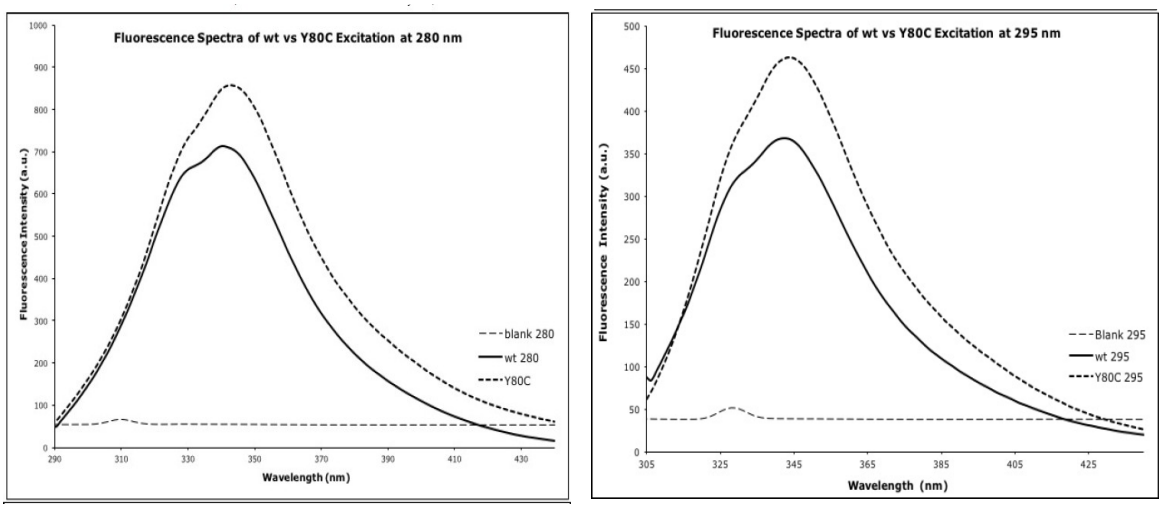

Figure 6. The resultant fluorescence spectra for the WT dimer (2 µM) (──) and mutant Y80C (2 µM) (- - -) in 20 mM sodium phosphate buffer pH 7.4, containing 1 mM EDTA and 0.02% (w/v) NaN are shown.

This observation is further supported by the thermal unfolding observations (Figure 7). We see that the mutants start to denature at a lower temperature (51 ± 3 ^{o}C and 47 ± 3 ^{o}C for P124A and Y80C, respectively) as compared to wildtype (55 ± 3 ^{o}C). This suggests that the hGSTP1-1 native protein is destabilised by changing the tyrosine-80 residue to cysteine.

CONCLUSIONS AND FUTURE WORK

Mutants P124A and Y80C were synthesised and structurally characterised for the hGSTP1-1 protein. The Y80C mutation has more effect on structural stability than the P124A mutation. As this is preliminary work, more data is required to understand the extent of this unfolding. Future work would include functional analysis (enzymatic activity) and solid state analysis by crystal structure.

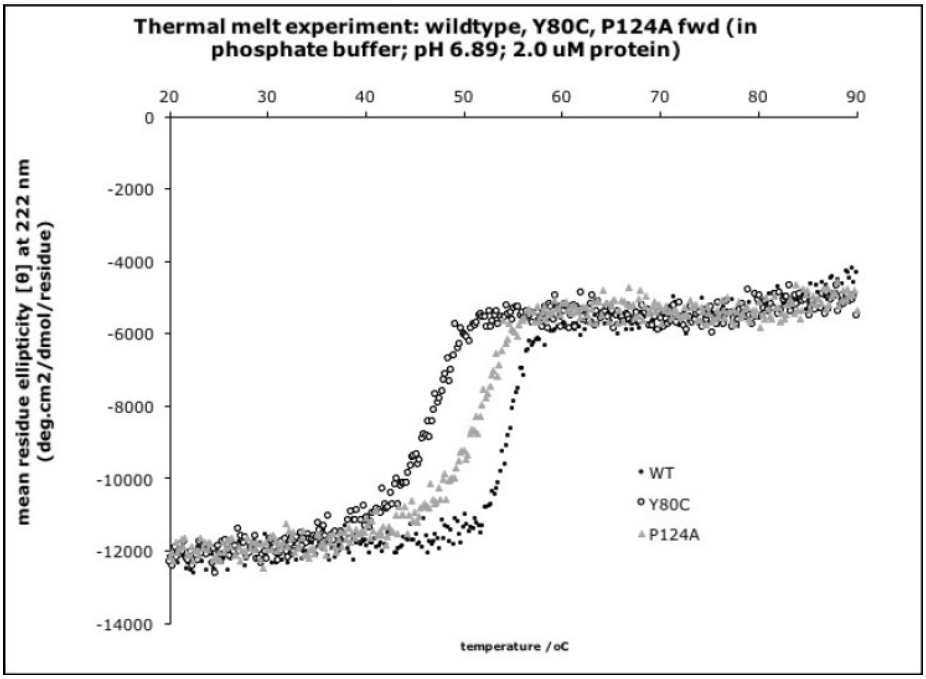

Figure 7. Far-UV CD spectra for the WT dimer (2 μM) (•); mutant Y80C (2 μM) (o) and P124A (2 μM) (Δ) as a function of temperature at a single wavelength. The CD spectra were measured at 222 nm with temperatures varying from 20 to 80^{o} C. Experiments performed in 20 mM sodium phosphate buffer pH 7.4, containing 1 mM EDTA and 0.02% (w/v) NaN3 are shown

Acknowledgements: *We are grateful to the National Research Foundation (NRF grant number: KICMA21), Department of Science and Technology (DST), and the Molecular Sciences Institute (MSI) administered by the University of the Witwatersrand, Johannesburg, South Africa, for funding this project and for the use of resources funded by these grants.*

REFERENCES

1. A. J. Oakley, *Curr. Opin. Struct. Biol.,* **15**, 716 (2005).
2. D. Sheehan, G. Meade, V. M. Foley, C. A. Dowd, *Biochem. J*, **360** (1), 1 (2001).
3. O. Vasieva, Curr. Mol. Med., **11**, 129 (2011).
4. R. N. Armstrong, *Chem. Res. Toxicol.,* **10**, 2 (1997).
5. D. M. Townsend, K. D., Tew, *Oncogene*, **22**, 7369 (2003).
6. hGSTP1-1 structure PDB ID: 2a2r: http://www.rcsb.org/pdb/
7. T. M. Buetler, D. J. Eaton, *Environ. Carcinogen. Ecotoxicol. Rev*., **C10**, 181 (1992).
8. K. D. Tew, Y. Manevich, C. Grek, Y. Xiong, J. Uys, D. M. Townsend, *Free Rad. Biol. Med.*, **51**(2), 299 (2011).
9. J. D. Hayes, R. C. Strange, *Pharmacology*, **61**, 154 (2000).
10. C. C. McIlwain, D. M. Townsend, K. D. Tew, *Oncogene*, **25**, 1639 (2006).
11. P.G. Board, Functional Genomics of the Human Glutathione Transferases, in: Encyclopedia of Drug Metabolism and Interactions, Wiley Online Library, 2012.
12. SNP database project: https://www.ncbi.nlm.nih.gov/snp/
13. U. M. Hezagyt, B. Mannervick, G. Stenberg, *J. Biol. Chem*., **279**, 9586 (2003).
14. M. Widersten, R. H. Kolm, R. Björnestedt, B. Mannervik, *Biochem. J.*, **285,** 377 (1992).
15. PrimerX software: http://bioinformatics.org/primerx
16. Z. Molaudzi, Structural and functional analysis of peroxiredoxin 6 and glutathione transferase P1-1, University of the Witwatersrand, Johannesburg, South Africa, dissertation, 2017.
17. BLAST software: https://blast.ncbi.nlm.nih.gov/Blast.cgi
18. 4Peaks software: https://nucleobytes.com
19. M. Chang, J. L. Bolton, S. Y. Blond, *Protein Expr. Purif*., **17**, 443 (1999).